Agricultural Systems 203 (2022) 103527

Contents lists available at ScienceDirect

Agricultural Systems

journal homepage: www.elsevier.com/locate/agsy

Identifying effective agricultural management practices for climate change adaptation and mitigation: A win-win strategy in South-Eastern Australia

Qinsi He [a,b,c], De Li Liu [c,d,*], Bin Wang [c,***], Linchao Li [a,c], Annette Cowie [e], Aaron Simmons [f], Hongxu Zhou [g], Qi Tian [a], Sien Li [h], Yi Li [i], Ke Liu [j], Haoliang Yan [k], Matthew Tom Harrison [j], Puyu Feng [l], Cathy Waters [m], Guangdi D. Li [c], Peter de Voil [n], Qiang Yu [a,o,**]

[a] State Key Laboratory of Soil Erosion and Dryland Farming on the Loess Plateau, Institute of Soil and Water Conservation, Northwest A&F University, Yangling, Shaanxi 712100, China
[b] School of Life Sciences, Faculty of Science, University of Technology Sydney, PO Box 123, Broadway, Sydney, NSW 2007, Australia
[c] NSW Department of Primary Industries, Wagga Wagga Agricultural Institute, Wagga Wagga, NSW 2650, Australia
[d] Climate Change Research Centre, University of New South Wales, Sydney, NSW 2052, Australia
[e] NSW Department of Primary Industries, Trevenna Rd, Armidale, NSW 2351, Australia
[f] NSW Department of Primary Industries, 98 Victoria St Taree, NSW 2430, Australia
[g] Department of Agricultural and Biological Engineering, University of Illinois at Urbana-Champaign, Urbana, IL 61801, USA
[h] Center for Agricultural Water Research in China, China Agricultural University, Beijing 100083, China
[i] College of Water Resources and Architectural Engineering, Northwest A&F University, Yangling 712100, China
[j] Tasmanian Institute of Agriculture, University of Tasmania, Newnham Drive, Launceston, Tasmania 7248, Australia
[k] State Key Laboratory of Cotton Biology, Institute of Cotton Research of the Chinese Academy of Agri-cultural Sciences, Anyang 455000, China
[l] College of Land Science and Technology, China Agricultural University, Beijing 100193, China
[m] NSW Department of Primary Industries, 34 Hampden Street, Dubbo, NSW 2830, Australia
[n] Queensland Alliance for Agriculture and Food Innovation (QAAFI), The University of Queensland, Gatton Campus, Gatton, QLD 4343, Australia
[o] College of Resources and Environment, University of Chinese Academy of Sciences, Beijing 100049, China

HIGHLIGHTS

- APSIM was used to simulate the effects of residue retention and crop rotation on GHG emissions and gross margins.
- Retaining all crop residues could turn the soil from a carbon source to a carbon sink, and benefit gross margins.
- Enhancement of residue retention on GHG abatement overweighed adverse effects of climate change under SSP245 and SSP585.
- The wheat-wheat-canola rotation was the most beneficial in terms of GHG mitigation and profitability compared with others.

GRAPHICAL ABSTRACT

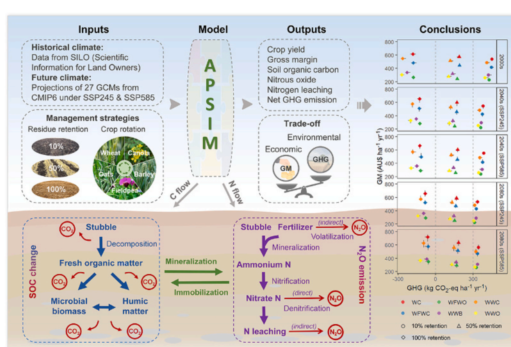

* Correspondence to: D. L. Liu, NSW Department of Primary Industries, Wagga Wagga Agricultural Institute, Wagga Wagga, NSW 2650, Australia.
** Correspondence to: Q. Yu, State Key Laboratory of Soil Erosion and Dryland Farming on the Loess Plateau, Institute of Soil and Water Conservation, Northwest A&F University, Yangling, Shaanxi 712100, China.
*** Corresponding author.
E-mail addresses: de.li.liu@dpi.nsw.gov.au (D.L. Liu), bin.a.wang@dpi.nsw.gov.au (B. Wang), yuq@nwafu.edu.cn (Q. Yu).

https://doi.org/10.1016/j.agsy.2022.103527
Received 20 April 2022; Received in revised form 21 September 2022; Accepted 22 September 2022

ARTICLE INFO

Editor: Kairsty Topp

Keywords:
Soil carbon sequestration
Nitrous oxide emission
Gross margin
Crop rotation
Residue retention
Climate change

ABSTRACT

CONTEXT: Farming systems face dual pressures of reducing greenhouse gas (GHG) emissions to mitigate climate change and safeguarding food security to adapt to climate change. Building soil organic carbon (SOC) is proposed as a key strategy for climate change mitigation and adaptation. However, practices that increase SOC may also increase nitrous oxide (N_2O) emissions, and impact crop yields and on-farm income. A comprehensive assessment of the effects of different management practices on trade-offs between GHG emissions and agricultural systems profitability under climate change is needed.

OBJECTIVE: We aimed to: (1) analyze the long-term trends of SOC and N_2O emissions, and ascertain whether the croplands of the study region are net GHG sources or sinks under climate change; (2) quantify the GHG abatement on a gross margin basis; (3) identify effective management practices that could achieve a win-win strategy; and (4) investigate sources of uncertainty in estimates of GHG emissions and gross margins under climate change.

METHODS: APSIM was used to simulate the effects of three crop residue retention rates (10%, 50% and 100%), and six representative crop rotations (wheat-canola, wheat-field pea-wheat-canola, wheat-field pea-wheat-oats, wheat-wheat-barley, wheat-wheat-canola, and wheat-wheat-oats) under two Shared Socio-economic Pathways scenarios (SSP245 and SSP585) using climate projections from 27 GCMs. GHG emissions and gross margins from 1961 to 2092 were assessed across 204 study sites in southeastern Australia.

RESULTS AND CONCLUSIONS: Our results showed that residue retention can turn the soil from a carbon source (10% retention, 304–450 kg CO_2-eq ha^{-1} yr^{-1}) to a carbon sink (100% retention, $-269 \sim -57$ kg CO_2-eq ha^{-1} yr^{-1}), and the potential of carbon sequestration was partly offset by concomitantly increased N_2O emissions. The wheat-wheat-canola rotation with full residue retention was shown to be a win-win solution with both large potential of GHG abatement and high gross margin compared with other rotations. Spatial analysis showed that the southeastern part of the study region, with higher rainfall, had higher gross margins, while the drier northwestern part had greater GHG emission reduction potentials. Although climate change led to increased GHG emissions and decreased yields for some crops, these adverse effects were overweighed by the higher SOC and yield advantages from full residue retention.

SIGNIFICANCE: This study emphasizes the significant potential for agronomic management to maximize gross margin and reduce GHG emissions under climate change in southeast Australia. Results from this study could be used by farmers and policymakers to mitigate climate change without compromising agroecosystem profitability.

1. Introduction

To meet the goal of the Paris Agreement to limit global warming to 1.5 °C above pre-industrial levels, both reductions of greenhouse gas (GHG) emissions and removal of atmospheric carbon dioxide (CO_2) are necessary (Field and Mach, 2017). Soil is a large carbon (C) reservoir in terrestrial ecosystems with a pool size of around 2400 Gt C (2 m depth), which is three times the amount of atmospheric carbon (Launay et al., 2021). Of the soil C pool, cropland soil plays a significant role in the global C budget, with a high and attainable mitigation potential of 1.4–2.3 Gt CO_2-eq yr^{-1} through improved management (Smith et al., 2019). According to the IPCC Special Report on Climate Change and Land, approximately 23% of global GHG emissions came from the agriculture, forestry and other land use (AFOLU) sector (Jia et al., 2019), and, without intervention, the anthropogenic GHG emissions from agriculture are projected to increase by 30–40% by 2050 (Mbow et al., 2019). To mitigate AFOLU GHG emissions, the international initiative "4 per 1000" that aims to increase global agricultural soil organic carbon (SOC) stocks through sustainable practices has been launched. The emphasis on increasing SOC has resulted in many studies conducted to assess the effects of different agricultural practices on SOC and promote various measures to enhance carbon sequestration (Farina et al., 2021; He et al., 2021; Lessmann et al., 2021; Rodrigues et al., 2021; Sándor et al., 2020).

Soil carbon sequestration is considered as one of the most important GHG mitigation opportunities for the agriculture sector, but its capacity can be overestimated if not assessed in a holistic manner as part of an integrated system (Harrison et al., 2021; Harrison et al., 2016; Meier et al., 2020b). For example, the retention of residue could not only increase the SOC but also increase the N_2O emissions via stimulating nitrification/denitrification and soil urease activity (Xia et al., 2018); longer crop rotations could impact multiple soil physicochemical and biological properties associated with releasing N_2O (Lehman et al., 2017) and building SOC (Renwick et al., 2021). Thus, the amount of N_2O emissions can determine whether the soils are net sinks or sources of GHG, depending on how other aspects of a system change under a given intervention (Christie et al., 2020; Ehrhardt et al., 2018). Moreover, the potential for SOC sequestration to continue is limited by the saturation ceiling, reflecting the capacity of soil to protect organic matter from decomposition (Lehmann and Kleber, 2015), but N_2O emissions continue each year (Lugato et al., 2018). Furthermore, SOC sequestration and N_2O emissions will be influenced differently by climate change-induced warming and rainfall variation (Meier et al., 2020b), since the microbial production of CO_2 and N_2O in soils have different sensitivities to temperature and moisture (Butterbach-Bahl et al., 2013). Therefore, the real mitigation effectiveness of C-sequestration management practices remains uncertain in space and time under climate change.

Greenhouse gas emissions mitigation and climate change adaptation must occur without compromising food security or causing loss of biodiversity, farm prosperity and social license to operate (Harrison et al., 2021). Altered management practices may impact food production and farmers' income (Dumbrell et al., 2017; Meier et al., 2020a), resulting in trade-offs between food security, GHG emissions, and farmer prosperity (Li et al., 2021b; Luo et al., 2017; Wang et al., 2018b; Xing et al., 2017). Recently, several practices intending to balance the trade-off between crop yields and GHG emissions, such as manure application, cover crop and no-tillage, have been assessed in China (Wang et al., 2018b), Europe (Quemada et al., 2020) and USA (Huang et al., 2022). In dry and hot environments such as experienced in Australian mainland cropping regions, the capacity for SOC sequestration is limited because of the high decomposition rates (high temperature promotes soil respiration) and low amount of crop residues (low rainfall reduces the organic matter inputs) (Liu et al., 2016). Combined with the uniquely variable and changing distribution of seasonal rainfall, Australia is facing great risks to crop productivity and profitability (Wang et al., 2022; Wang et al., 2018a). In New South Wales (NSW) and Queensland cropping systems, the climate variability over the past 20 years contributed to a 36% decline in profits on average (relative to 1950–2000) and this trend is expected to continue (Wood et al., 2021). Understanding the relationships among crop profitability, GHG emissions, and climate change is essential for designing improved management practices that offer win-win-win in terms of productivity, profitability and GHG emissions (Harrison et al., 2021). The GHG emissions per unit farm gross margin (in other words, the gross margin-scaled emissions) is a useful indicator to contrast the GHG impacts of the cropping system without neglecting the economic performance, especially for multi-crop rotation systems where different crops have different economic values (Li et al., 2017).

Alternative management practices can affect SOC sequestration, N_2O emissions, and crop profitability simultaneously. Although numerous studies have assessed the effects of management practices, most of them focus on one aspect only, leaving the integrated effects of practices poorly understood. For example, Mohanty et al. (2020) found that nutrient management helped to turn soils into C sinks by increasing SOC stocks, but the possible concomitant increase in N_2O emission was not considered. In addition, although many field experiments have been conducted to assess the effects of agricultural practices on soil gas fluxes and crop growth, few practices can be evaluated in an individual field experiment, and these results cannot readily be extrapolated to regional scales due to variation in climate, soil type, management and other. Moreover, the trade-offs between GHG emissions and gross margins are not often reported and the interactions between climate change and management interventions are rarely considered over long time-scales (Huang et al., 2022).

In this study, we used APSIM to simulate the economic performance and net GHG emissions for a range of on-farm practices under climate change across a cropping region in southeastern Australia. We aimed to: (1) analyze the trends of SOC and N_2O emissions, and ascertain whether the agricultural soils of the study region are net GHG sources or sinks under climate change; (2) quantify the GHG abatement on the gross margin basis; (3) identify effective management practices that could achieve a win-win strategy; and (4) investigate sources of uncertainty in estimates of GHG emissions and gross margins under climate change.

2. Materials and methods

2.1. Study area

The 204 sites selected for this study were distributed across the cropping area in the Riverina region of NSW, in south-eastern Australia (Fig. 1a), which is responsible for a large proportion of Australia grain production. The region is characterized by a semi-arid climate with a long-term annual rainfall of 477 mm and an average temperature of 16.5 °C (Fig. 1b-c). The main soil types are Chromosols, Dermosols, and Vertosols (Isbell and National Committee on Soil and Terrain, 2021). Agriculture is the major economic activity and the region generates 12.7% of all agricultural production in NSW (Department of Planning and Environment, 2017). Wheat, barley, and canola are the three major crops grown in this region. However, increasingly frequent extreme weather events, such as drought and heat waves are likely to continue to pose economic and environmental challenges on many agricultural sectors in this region (Chang-Fung-Martel et al., 2017).

2.2. Climate and soil data

Daily climate data comprising global solar radiation, rainfall, maximum and minimum temperature were required to drive the crop model. The historical climate data during 1900–2020 at the 204 study sites were downloaded from SILO-patched point dataset (Scientific Information for Land Owners) (https://www.longpaddock.qld.gov.au/silo/) (Jeffrey et al., 2001). For future climate scenarios, we selected two SSPs to represent an intermediate "middle of the road" scenario (SSP245) and a high emissions "fossil-fueled development" scenario (SSP585) (O'Neill et al., 2016). Basic information for 27 available GCMs

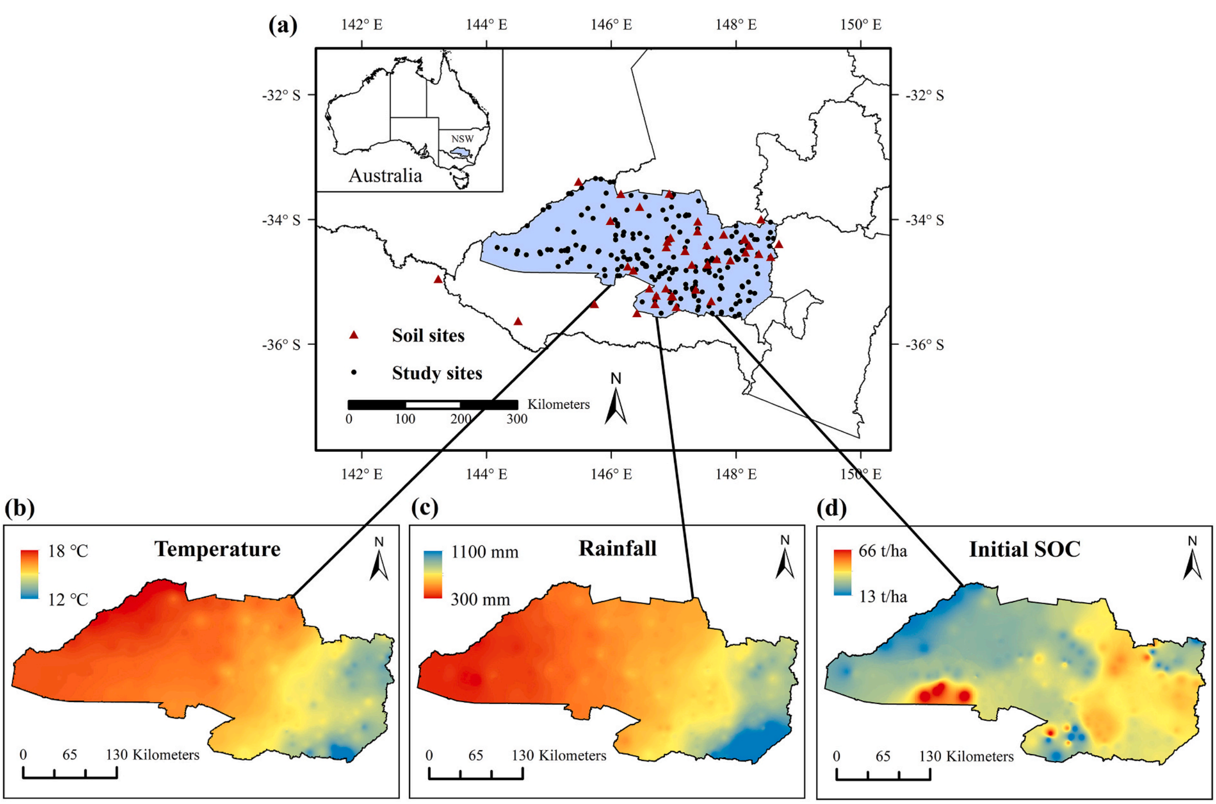

Fig. 1. Locations of the Riverina region, 204 study sites and 41 soil sites in southern New South Wales (NSW) in southeastern Australia (a), the average historical climate during 1985 to 2020 (b-c), and the average SOC content before implementing management practices during 1958 to 1960 (d). The spatial distributions (b-d) were interpolated using inverse distance weighting method (IDW).

from the Coupled Model Intercomparison Project Phase 6 (CMIP6, https://pcmdi.llnl.gov/CMIP6/) is presented in Table S3. As APSIM input requires daily climate data but raw GCMs are at coarse temporal (monthly) and spatial (100–300 km grid solution) resolutions, these gridded data were downscaled to each study site using the method developed by Liu and Zuo (2012). The statistical downscaling model involved three steps. In the first step, the gridded monthly GCM data in 1900–2100 were spatially downscaled to each of 204 weather stations using the inverse distance weighting method (IDW). The second step was the bias-correction of the GCM data towards the observed climate data for each site by using the quantile mapping technique. In the third step, the monthly bias-corrected data were disaggregated to daily data using a modified version of the WGEN stochastic weather generator (Richardson and Wright, 1984).

We used soil data from APSoil database (http://www.asris.csiro.au/mapping/hyperdocs/APSRU/), which contains information including soil description, soil classification, site, region, country, latitude, longitude, and data source recording the experiments from where the soil was sampled (Dalgliesh et al., 2012). Each soil dataset has the layer-wise parameters including bulk density, organic carbon, saturate water content, crop specified lower limit, and drained upper limit. Some other parameters such as soil pH, electrical conductivity, chloride and exchangeable cations are also recorded for some profiles. This database was constructed for the explicit purpose of providing input soil parameters required for running APSIM. Soils that were identified to be geographically closest to our study sites were ultimately selected (Fig. 1a). Using the closest soil data for each site could reduce the bias from using an unrepresentative soil in spatial analysis, and this method had been used in many other crops modelling studies in Australia (Feng et al., 2020; Wang et al., 2019b).

2.3. APSIM model

The Agricultural Production Systems Simulator (APSIM, version 7.10) (Keating et al., 2003) is a process-based biophysical model, and has been widely used to simulate crop growth and soil processes in response to management practices and/or environmental change (Li et al., 2021b; Liu et al., 2017; Liu et al., 2020; O'Leary et al., 2016; Wang et al., 2019a). In APSIM Classic, the SoilN module simulates SOC dynamics on a daily time step, coupling with modules of SoilWat/SWIM (soil moisture), SurfaceOM (surface organic matter), and crop modules. Soil organic matter (SOM) is divided into three conceptual pools, namely fresh organic matter (FOM), microbial biomass (BOM), and humic pool (HUM). The FOM pool has three types of organic matter including carbohydrate, cellulose, and lignin. The BIOM pool contains the soil microbial biomass and microbial products. The HUM pool contains the rest of the SOM, and a fraction of HUM is considered indecomposable (inert carbon). Decomposition of each pool is treated as a first-order decay process modified by temperature, moisture, and nutrient availability (Probert et al., 1998). Simulation of the decomposition of crop residues takes into account the degree of contact between residues and soil to modify the maximum potential decomposition rate (Thorburn et al., 2001). Crop residues can be burnt, removed from the system, incorporated into soil or left at the surface for decomposition, as specified in Manager and SurfaceOM modules. Retention of residues via tillage moves the surface residues directly into the FOM pool, thereafter resulting in C transfer to other pools and the release of CO_2 to the atmosphere.

Daily N_2O emissions from soil are simulated as the sum of N_2O emissions from daily denitrification and nitrification. Denitrification rates (R_{denit}, kg N ha^{-1} day^{-1}) are estimated as a function of the denitrification coefficient (K_{denit}, = 0.001379), the amount of NO_3^- in soil (NO_3-N, kg N ha^{-1}), active carbon (C_A, ppm), and the limiting factors (scaled from 0 to 1) for soil temperature (T) and moisture (M), which can be expressed as (Thorburn et al., 2010):

$$R_{denit} = K_{denit} \times NO_3^- \times C_A \times f(T) \times f(M) \tag{1}$$

N_2O emissions during denitrification are then calculated by combining the denitrification rate with the ratio of N_2 to N_2O emitted during denitrification predicted by the model of Del Grosso et al. (2000). Simulation of the nitrification rate (R_{nit}, kg N ha^{-1} day^{-1}) follows the Michaelis-Menten response to available soil ammonium (NH_4, mg kg^{-1}), and is modified by soil temperature (T), moisture (M), and pH, represented as:

$$R_{nit} = K_{max} \times \frac{NH_4}{NH_4 + K_{NH_4}} \times f(T) \times f(M) \times f(pH) \tag{2}$$

where, K_{max} is the maximum nitrification rate and K_{NH_4} is the NH_4 concentration for half the maximum reaction velocity. N_2O emissions during nitrification are calculated as a proportion of nitrified N (0.2%) (Li et al., 2007). A detailed description of the method used in APSIM to simulate N_2O emissions from soil is given by Thorburn et al. (2010).

2.4. Model validation and scenario analysis

The performance of APSIM in simulating crop yields (Meier et al., 2020a; Wang et al., 2018b; Yan et al., 2020), SOC dynamics (Godde et al., 2016; Luo et al., 2011; O'Leary et al., 2016), and N_2O emissions (Bilotto et al., 2021; Mielenz et al., 2016; Thorburn et al., 2010) has been widely and explicitly tested and verified under different cropping systems, and could be applied for various rotation systems (Hochman et al., 2020). In this study, we used the previously calibrated and validated varieties in each crop module released by APSIM. Similar to some regional modelling studies (Choi et al., 2021; Jin et al., 2022; Kheir et al., 2021), we further evaluated the ability of APSIM in simulating SOC, N_2O and crop yields, using the experimental data collected at Wagga Wagga site before the simulation for all sites. We also compared our simulated yields with the regional average from Yield Gap (https://yieldgapaustralia.com.au/maps/). Specifically, the SOC and wheat yields were validated using data from a long-term experiment (SATWAGL) conducted from 1979 to 2004 at Wagga Wagga (Liu et al., 2009). N_2O emissions were validated using experimental data from Li et al. (2016); Li et al. (2021a); and Li et al. (2018). Details of the two experiments and APSIM performance are provided in supplementary material. To evaluate the model performance, we used root mean squared error (RMSE) and mean absolute percentage error (MAPE) to measure the difference between predicted and observed values as follows:

$$RMSE = \sqrt{\frac{1}{n}\sum_{i=1}^{n}(P_i - O_i)^2} \tag{3}$$

$$MAPE = 100\% \times \frac{1}{n}\sum_{i=1}^{n}\left|\frac{P_i - O_i}{O_i}\right| \tag{4}$$

where, P_i and O_i are the predicted and observed values, and n is the number of samples.

As the SOC recorded in the APSoil database for each site represents different cropping histories and farming management at the time of the data collected, it was necessary to establish a comparable initial SOC level for each site to enable an unbiased comparison of the spatial-temporal changes across different managements. To achieve this, APSIM was run at the 204 sites from 1920 to 1960 for a continuous wheat cropping system with 50 kg N ha^{-1} at sowing and 25% retention of wheat residues. The rate of retention represents a farming practice with most of the residues removed from the field and the N application amount is the rate typically applied across the study area. The accumulation of SOC could reach a steady state after the 41-year spin-up period (O'Leary et al., 2016), and the outputs were used as the initial values for following 132-year simulation. From 1961 to 2092, APSIM was used to simulate six crop rotations: wheat-canola (WC), wheat-field pea-wheat-canola (WFWC), wheat-field pea-wheat-oats (WFWO), wheat-wheat-barley (WWB), wheat-wheat-canola (WWC) and wheat-wheat-oats (WWO), which were chose based on crop rotations practiced in this region. For each rotation, we set three residue retention rates: 10% (removing stubble from simulation, i.e., typical burning practices in the study region), 50% (removing half of the stubble), and 100% (retaining all stubble from the previous year). Fertilizer application for field pea was 10 kg N ha^{-1} at sowing, while for cereals and canola, fertilizer N amount varied with the average precipitation of each site using a fitted relationship (Simmons et al., 2022):

$$N = \frac{(WU - A) \times C}{WU - B} \tag{5}$$

where, *WU* is the sum of the precipitation during growing season and one quarter of the precipitation during fallow period at each study site. *A*, *B*, and *C* are coefficients. The amount of N applied at sowing was calculated by $A = 150$, $B = 10$ and $C = 25$ for all crops. The total N applied (sum of N application at sowing and top dressing) was calculated by $A = 150$ and $B = 90$ for all crops, while $C = 108$, 130, 80 and 64.8 for wheat, canola, barley and oats, respectively. The total N application in the range from 43 to 121 kg N ha^{-1}, representing the local farming practices under rainfed conditions.

The sowing times and the length of sowing windows were set according to the NSW Department of Primary Industries sowing guidelines (Matthews et al., 2015). Different sowing windows were set for wheat (15 March to 30 June), barley (15 April to 15 July), canola (8 April to 15 June), field pea (1 May to 30 June), and oats (1 May to 22 June). We used two generic cultivars for each site: a longer season "winter-type" was used when crop was sown before the mid-point of the sowing window, and a shorter season "spring-type" was used when crop was sown after the mid-point of the sowing window (Liu et al., 2016). The soil water requirement for sowing was nonlinearly declined from 1.2 plant available water capacity (PAWC) for the start of the sowing-window to 0.8 PAWC at the end of the sowing-window. If soil water that met the criteria was less than PAWC, crop was sown on the same day, otherwise, sowing date was delayed by 1 day (1.0–1.1 PAWC), 2 days (1.1–1.2 PWAC) or 3 days (>1.2 PAWC). If these sowing criteria were not met, crop was sown at the end of the sowing-window. In addition, the APSIM also requires atmospheric CO_2 concentrations to simulate crop growth. We calculated $[CO_2]$ for SSP245 and SSP585 following the approach used by Bai et al. (2022):

$$\begin{aligned}[CO_2]_{SSP245} = {} & 62.044 + \frac{34.002 - 3.8702y}{0.24423 - 1.1542y^{2.4901}} + 0.028057 \times (y - 1900)^2 \\ & + 0.00026827 \times (y - 1960)^3 - 9.2751 \times 10^{-7} \times (y - 1910)^4 \\ & - 2.2448 \times (y - 2030)\end{aligned} \tag{6}$$

$$\begin{aligned}[CO_2]_{SSP585} = {} & 757.44 + \frac{84.938 - 1.537y}{2.2011 - 3.8289y^{-0.45242}} + 2.4712 \times 10^{-4} \\ & \times (y + 15)^2 + 1.9299 \times 10^{-5} \times (y - 1937)^3 + 5.1137 \times 10^{-7} \\ & \times (y - 1910)^4\end{aligned} \tag{7}$$

where, y is the calendar year from 1920 to 2092 (i.e., y = 1920, 1921, …, 2092).

2.5. Greenhouse gas emissions and gross margins

To assess the long-term impacts of management practices on soil GHG emissions and gross margins, APSIM was continuously run from 1961 to 2092. The 132-year simulation was used because a 36-year period can provide full rotation cycles for all six rotations, i.e., 18, 12, and 9 full rotation cycles for the two-year (WC), three-year (WWB, WWC, and WWO) and four-year rotations (WFWC and WFWO), respectively. Downscaled climate projections of 27 GCMs under SSP245 and SSP585 were used. In total, we ran 198,288 simulations (204 sites × 27 GCMs × 2 climate scenarios × 6 rotations × 3 residue retentions). Each simulation quantified the GHG flux in CO_2 equivalents (CO_2-eq), which was calculated as the sum of soil CO_2 and N_2O fluxes using 100-year global warming potential (GWP) of 273 for N_2O according to AR6 (Forster et al., 2021):

$$GHG = 273 \times N_2O - \Delta SOC \times 44/12 \tag{8}$$

where, ΔSOC is the difference between the SOC (0-30 cm) after t years (from 1 to 132 years) of the simulation and the initial SOC content. Positive and negative values of GHG indicate that the soil is a net sink and source of atmospheric CO_2, respectively. N_2O emissions are estimated as the sum of direct emissions from soil via nitrification and denitrification processes (predicted by APSIM as specified above, N_2O_d) and indirect emissions from atmospheric deposition of N volatilized from soil as well as from N leaching/runoff. For the indirect emissions resulting from N volatilization, we adopted the IPCC approach as Hergoualc'h Hergoualc'h et al. (2019):

$$N_2O_V = N \times F_V \times \mathrm{EF}_V \times 44/28 \tag{9}$$

where, *N* is the annual amount of fertilizer being applied (kg N ha^{-1} yr^{-1}), F_V (= 0.11) is the fraction of total N input that is volatilized as NH_3 and NO_X (kg N volatilized per kg N applied), EF_V (= 0.01) is the emission factor for N_2O emission resulting from N volatilization (kg N-N_2O per kg N volatilized). Emissions from N leaching/runoff were similarly estimated using the IPCC approach (Hergoualc'h Hergoualc'h et al., 2019):

$$N_2O_L = N_L \times EF_L \times 44/28 \tag{10}$$

where, N_L is the amount of N leaching/runoff which is estimated by the APSIM model (kg N ha^{-1} yr^{-1}), and EF_L (= 0.011) is the emission factor for N_2O emission resulting from the N leaching/runoff (kg N-N_2O per kg N leached/runoff). Thus, the total N_2O emissions were calculated as:

$$N_2O = N_2O_d + \mathrm{N_2O}_V + N_2O_L \tag{11}$$

To compare the six rotations, the income of each crop was estimated using gross margins (GM, AU\$ ha^{-1} yr^{-1}), that were calculated using the method given in Li et al. (2017) and Xing et al. (2017):

$$GM = (GI - C_S - C_T - C_F - C_H - C_I) \times (1 - L) \tag{12}$$

where, GI is the on-farm grain income estimated as the on-farm price (\$ t^{-1}) multiplied by crop yield (t ha^{-1}). L is the government levy (%). C_S, C_T, C_F, C_H and C_I are the costs for sowing, tillage, fertilizer, harvest and pest control, respectively (\$ ha^{-1}). The on-farm price for each crop is

Table 1
Details of economic costs of agricultural management for wheat, barley, canola, field pea, oats and the on-farm prices used to calculate gross margins of these five crops.

Variable costs	Unit	Wheat	Barley	Canola	Field pea	Oats
Income						
On-farm grain price	\$ t^{-1}	317	243	757	400	204
Cost						
Cultivation	\$ ha^{-1}	0	0	17	6	38
Sowing	\$ ha^{-1}	30.2	28.7	47.2	100.9	33.6
Fertilizer	\$ ha^{-1}	72.5	58.5	108.7	37.6	40.0
Pest control	\$ ha^{-1}	80.7	67.6	61.7	90.6	56.2
Harvest[a]	\$ ha^{-1}	50.5	37.0	52.0	49.4	37.1
Levies	%	1.02	1.02	1.02	1.02	1.02

Data are from DPI gross margin budgets (https://archive.dpi.nsw.gov.au/).
[a] The prices of harvest are for the first 2.5 t of grain yield, beyond which a factor of 0.01 is multiplied.

given in Table 1. Costs and calculations were coded in the Manager module of APSIM. Thus, GMs for the rotations were calculated as the sum of the single crop gross margins in each treatment. When studying the trade-offs between GHG mitigation and GM, emissions from tractor use associated with each operation were also considered. Fuel use for sowing, spraying, spreading, harvesting and grain collection were estimated as 4.4, 0.7, 1.15, 5.8 and 2.1 L ha^{-1} according to the AusAgLCI (Grant et al., 2014), with emissions of 2.7174 kg CO_2-eq per liter of fuel burned (NGA, 2021).

2.6. Secondary bias correction of simulation outputs

The statistical downscaling model procedure we used in this study was applied to correct stationary bias and systemic errors in the GCM data (Liu and Zuo, 2012). Theoretically, a perfect procedure could generate downscaled climate data that are the same as the observations. Consequently, the APSIM model outputs driven by the downscaled data should be the same as the outputs driven by observations. However, due to imperfections in the bias correction and non-stationary biases in the GCM data, there are some differences between the simulation outputs driven by downscaled GCM data and by climate observations for the historical period. These differences can be corrected, denoted as a secondary bias correction (SBC) procedure after the bias correction in the downscaling procedure (Liu et al., 2017). Therefore, prior to the analysis of soil GHG emissions and crop gross margins, all the APSIM outputs driven by the downscaled climate data were subjected to SBC as (Yang et al., 2016):

$$X = X_G - \left(\overline{X}_{G_{bl}} - \overline{X}_{O_{bl}}\right) \tag{13}$$

where, X is the value after correction, X_G is the value from APSIM simulation driven by downscaled GCM data, $\overline{X}_{G_{bl}}$ and $\overline{X}_{O_{bl}}$ are the mean values over a historical baseline period driven by GCM data and observed climate data, respectively. In this study, we used the period from 1961 to 2020 as the historical baseline period and all following analyses are based on the corrected values.

2.7. Analyses and partitioning uncertainty

We assessed the uncertainties in soil GHG emissions and gross margins due to 27 GCMs, two SSPs with two future periods (SSP245 for the 2040s, SSP245 for the 2080s, SSP585 for the 2040s, and SSP585 for the 2080s), and their interaction for each residue retention rate using the ANOVA method following Wang et al. (2020). The total uncertainty can be expressed as:

$$SST = SS_{SSP} + SS_{GCM} + SSI \tag{14}$$

where, SST is the total sum of the squares, SS_{SSP} and SS_{GCM} are the sum of squares due to the two main factors, and SSI is their interaction (SSP × GCM). In this study, we used the percentages of these three sources to compare their contributions to total uncertainty.

3. Results

3.1. Model performance

The APSIM model simulated SOC change reasonably well in the 0–30 cm soil layer for the SATWAGL experiment at Wagga Wagga from 1979 to 2004. The RMSE (root mean square error) ranged between 1.3 and 2.5 t C ha^{-1}, and MAPE (mean absolute percentage error) ranged between 2.6 and 5.3% (Fig. S1a-d). Despite large inter-annual variation in SOC observations, APSIM captured the declining trend in SOC well. APSIM was also well constrained for simulating the observed N_2O emissions in the top 30 cm soil layer, with a RMSE of 0.02 kg N ha^{-1} and MAPE of 11.3%, although the N_2O data were very limited (Fig. S1e). In addition, the observed wheat yield of the SATWAGL experiment during 1979–2002 was 3.26 t ha^{-1} on average, and the average simulated wheat yields in the same period were 2.99, 3.13 and 3.32 t ha^{-1} under 10%, 50% and 100% residue retentions, respectively (Fig. S1f). The average yields of different crops over the study region were also compared with the data from an open database, in which the simulated yields were similar to the actual yields for wheat and barley but close to the water-limited yields for canola (Fig. S2).

3.2. Temporal trend of cumulative soil fluxes

For the SSP245 scenario, when 10% residue was retained, SOC stock decreased gradually and soil released CO_2 into the atmosphere (Fig. 2A a-f), with cumulative emissions of 15.8, 24.5 and 30.6 t CO_2-eq ha^{-1} across six rotations during the 2000s, 2040s and 2080s, respectively (Table S4). The cumulative N_2O emissions were relatively small compared to the SOC loss, with average values of 0.6, 0.8 and 0.9 t CO_2-eq ha^{-1} during the three periods, respectively. Under this residue management, average net GHG flux increased up to 31.6 t CO_2-eq ha^{-1} by 2080s, in which WWO had the lowest emission of 30.3 t CO_2-eq ha^{-1}, and WC had the highest emission of 33.7 t CO_2-eq ha^{-1} (Table S5).

When 50% of residue was retained, inputs of C provided by crop residues were still inadequate to compensate for decomposition loss, resulting in a net loss of SOC and positive net GHG emissions (Fig. 2A g-l). Compared with the 10% retention, the cumulative CO_2 emission from soil decreased to 10.3 t CO_2-eq ha^{-1}, while N_2O emission increased to 2.0 t CO_2-eq ha^{-1} by the 2080s. Consequently, net GHG emissions fell by more than half in the 10% retention treatment, with an average value of 12.2 t CO_2-eq ha^{-1} (Table S4). Similar to 10% residue retention, the WC rotation had the highest GHG emission of 14.6 t CO_2-eq ha^{-1}, while WWO contributed the least GHG of 8.7 t CO_2-eq ha^{-1} by 2080s (Table S5).

When 100% residue was retained, all of the six rotations switched from carbon sources to carbon sinks. Although the N_2O emissions quadrupled during the whole period compared with 10% retention treatment, SOC sequestration was great enough to completely offset the additional N_2O emissions, thus the cumulative soil GHG fluxes were always negative (Fig. 2A m-r). The SOC stocks for all rotations increased asymptotically until the 2040s, reaching a new steady-state equilibrium, and thereafter the sequestration rates slowed down. For example, the amounts of SOC sequestration in WWB increased from 12.3 t CO_2-eq ha^{-1} during 2000s to 17.9 t CO_2-eq ha^{-1} during 2040s, but for the following 36 years the sequestration only reached 19.5 t CO_2-eq ha^{-1} by 2080s. The gradually saturated SOC and cumulative N_2O emissions finally caused inflection points of net GHG fluxes, that is, GHG removal of WWB was −15.3 t CO_2-eq ha^{-1} by the 2040s, but decreased to −15.0 t CO_2-eq ha^{-1} by the 2080s (Table S5). However, the SOC content in WWO increased steadily until the end of the simulation with low N_2O emissions, showing the largest potential of GHG removal of −20.5 t CO_2-eq ha^{-1} by the 2080s (Fig. 2A r).

For the SSP585 scenario, simulated outcomes from all rotations were consistent with those under SSP245 scenario (Fig. 2B). Specifically, WC with 10% and 50% residue retention had the largest cumulative net GHG emissions, releasing up to 34.7 and 16.5 t CO_2-eq ha^{-1} by 2080s, respectively. WWO emitted the least GHG of 31.5 and 10.4 t CO_2-eq ha^{-1} under 10% and 50% retention respectively, and removed the most GHG (−18.2 t CO_2-eq ha^{-1}) under 100% retention by 2080s (Table S5). However, the mitigation potential of all treatments was reduced under SSP585 compared to SSP245. It is noteworthy that, although GHG emissions were always negative when 100% residue was retained, the benefits of SOC sequestration would be partly negated by N_2O emissions. The net mitigation increased until around the 2040s, after which the mitigation potential decreased.

3.3. Trade-offs between GHG and GM

When 10% and 50% residues were retained, the average annual GHG

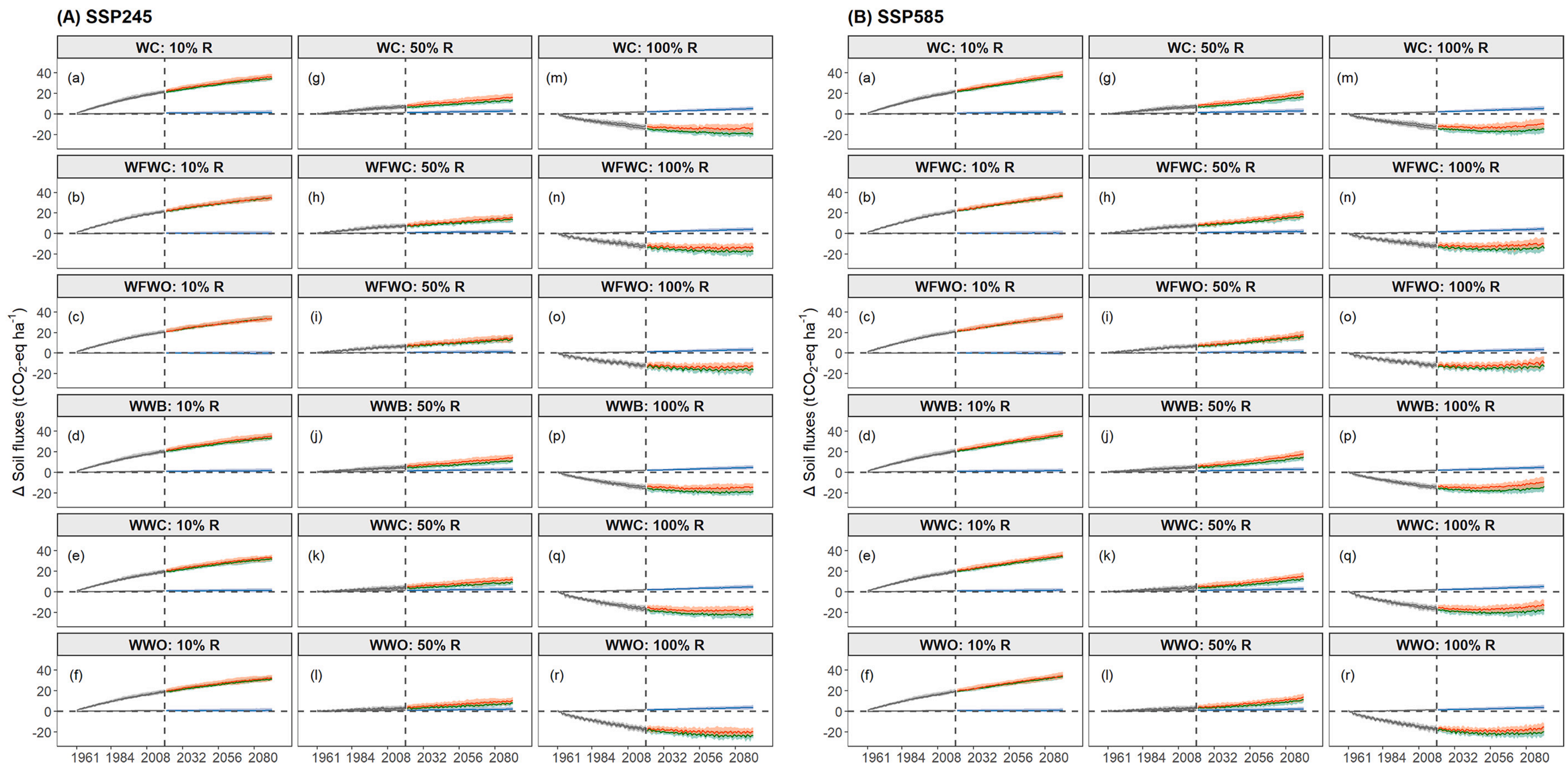

Fig. 2. Temporal trend of cumulative CO_2 emissions from soil (green lines), N_2O emissions (blue lines) and net GHG soil fluxes (orange lines) over six rotations (WC, wheat-canola; WFWC, wheat-field pea-wheat-canola; WFWO, wheat-field pea-wheat-oats; WWB, wheat-wheat-barley; WWC, wheat-wheat-canola; and WWO, wheat-wheat-oats) and three residue retention rates (10%, 50%, and 100%) during historical (gray lines, 1961–2020) and future (2021–2092) periods under SSP245 (A) and SSP585 (B). The lines are the median values, and the shaded areas are the 10th and 90th percentiles of APSIM simulations based on 27 GCMs. Negative and positive values indicate an atmospheric sink and source, respectively. (For interpretation of the references to colour in this figure legend, the reader is referred to the web version of this article.)

emissions of WWO were always lower than other rotations, and WC had relatively higher annual values (Fig. 3A a-d). The differences among rotations became more pronounced under 100% retention, in which average annual GHG emissions were negative for all rotations, WC, WFWC and WFWO had the lowest annual GHG removals, while WWC and WWO had the highest values (Fig. 3A e-f). With respect to the average annual GHG emissions of historical simulations for 1985–2020, GHG emissions decreased with time under 10% retention, while removals decreased over time under 100% retention. GHG emissions differed little between climate change scenarios.

The WC rotation, which always showed the largest annual GHG emissions, also had the highest gross margin, while the WWO had both the lowest GHG emission and gross margin (Fig. 3B). For example, with 100% retention under SSP585 scenario, gross margins of WC and WWO were 719 and 365 AU\$ ha^{-1} yr^{-1} in 2080s, respectively, with net GHG removals of −62 and − 122 kg CO_2-eq ha^{-1} yr^{-1}, respectively (Table S6). In addition, residue retention increased gross margins under both SSP245 and SSP585 scenarios. For example, the gross margins of WWO were 265, 305 and 365 AU\$ ha^{-1} yr^{-1} in 2080s under 10%, 50%, and 100% retention, respectively (Table S6).

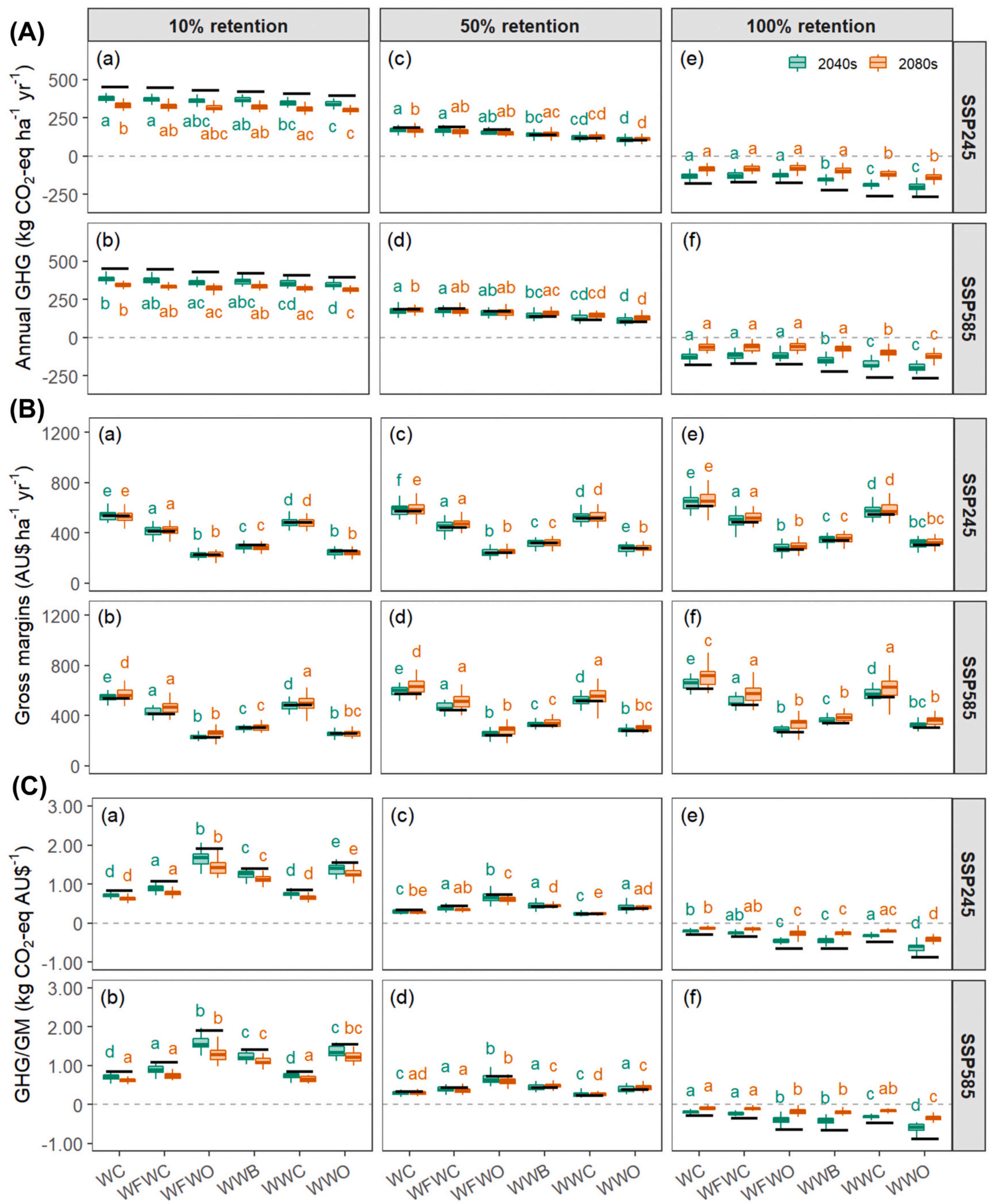

Fig. 3. Effects of management practices on annual GHG (A), GM (B) and GHG/GM (C) during 2021–2056 (2040s) and 2057–2092 (2080s) under SSP245 and SSP585 scenarios. Horizontal black lines represent the average historical values (1985–2020). Each box summarizes 27 values of the APSIM simulations based on 27 GCMs. Boxplots show the median, and the 25th and 75th percentiles. Different letters indicate significant differences between groups with Tukey post-hoc test ($p < 0.05$). Green and orange letters denote significant differences during the 2040s and 2080s, respectively, and no comparison was done between the two periods. Crop rotation abbreviations are defined in Fig. 2. (For interpretation of the references to colour in this figure legend, the reader is referred to the web version of this article.)

The GM-scaled GHG emissions of WFWO, WWB, and WWO were significantly higher than other rotations, and those of WC and WWC were the lowest under 10% and 50% residue retention (Fig. 3C a-d). For example, the GM-scaled GHG emission of WC was 0.63 kg CO_2-eq. AU $\$^{-1}$ with 10% retention in 2080s under SSP585, which was half of the WWO with 1.22 kg CO_2-eq. AU$\$^{-1}$ (Table S6). Under 100% residue retention, WC and WFWC had larger values of GHG/GM, while WWO had the most negative GHG/GM. Overall, WC had the highest gross margins and WWO had the greatest GHG abatement, WWC could achieve both high gross margin and large potential for GHG removal (Fig. 4).

3.4. Spatial pattern of GM-scaled GHG

Spatially, the southeastern part of the study region always had greater GHG emissions from all rotations than those of the northwestern region (Fig. S3). The whole region was a carbon source under 10% retention and a carbon sink under 100% retention. Furthermore, we found that under 50% residue retention with the same rotation, the southeastern region was a carbon source but the northwestern region was a carbon sink (Fig. S3g-l). However, the GM showed the opposite spatial patterns, decreasing from east to west, and this trend became more obvious with increasing residue retention (Fig. S5). Therefore, the GM-scaled GHG were less positive (with 10% retention) and more negative (with 50% and 100% retention) in the north-west compared to the south-east, though a small southwestern part showed large GHG emissions per unit of GM (Fig. 5). Overall, the northwestern region performed better in GHG abatement, while the southeastern region showed higher gross margins, and the whole region showed benefits from residue retention.

3.5. Sources of uncertainty

Since the WWC rotation was optimal in terms of the trade-off between GHG and GM, we analyzed the contributions of SSP, GCM and their interaction to the total uncertainty in simulating annual GHG emissions and GM under each residue retention rate (Fig. 6). For annual GHG, SSP was the major source of uncertainty under 100% residue retention (64%), while the contribution decreased to 43% and only 9% under 10% and 50% retention, respectively. Conversely, GCM contributed the least of 29% and the most of 74% to total uncertainty in simulating GHG under 100% and 50% residue retention, respectively (Fig. 6a). For GM, GCM contributed the most to total uncertainty independent of residue retention rates, with contribution rates ranging from 64% to 66% (Fig. 6b). The interaction of GCM and SSP was also an important source of uncertainty in simulating GM, accounting for 31–32%. In contrast to GHG, SSP was the smallest source of uncertainty for GM, with negligible contributions of only 2–6%.

4. Discussion

4.1. Responses of SOC to management practices

Residue retention is widely considered to be one of the most sustainable and economically viable management practices for sequestering atmospheric CO_2 and improving global C storage in agricultural soils (Jin et al., 2020; Paustian et al., 2016). Our simulation results demonstrated that residue retention in dryland crops significantly decreased net GHG emissions, mainly due to the enhanced SOC sequestration especially in the northwestern part of the Riverina region (Fig. 2 and Fig. S3). This result can be explained by the lower initial SOC content in northwest than in southeast (Fig. 1d). In general, the rate at

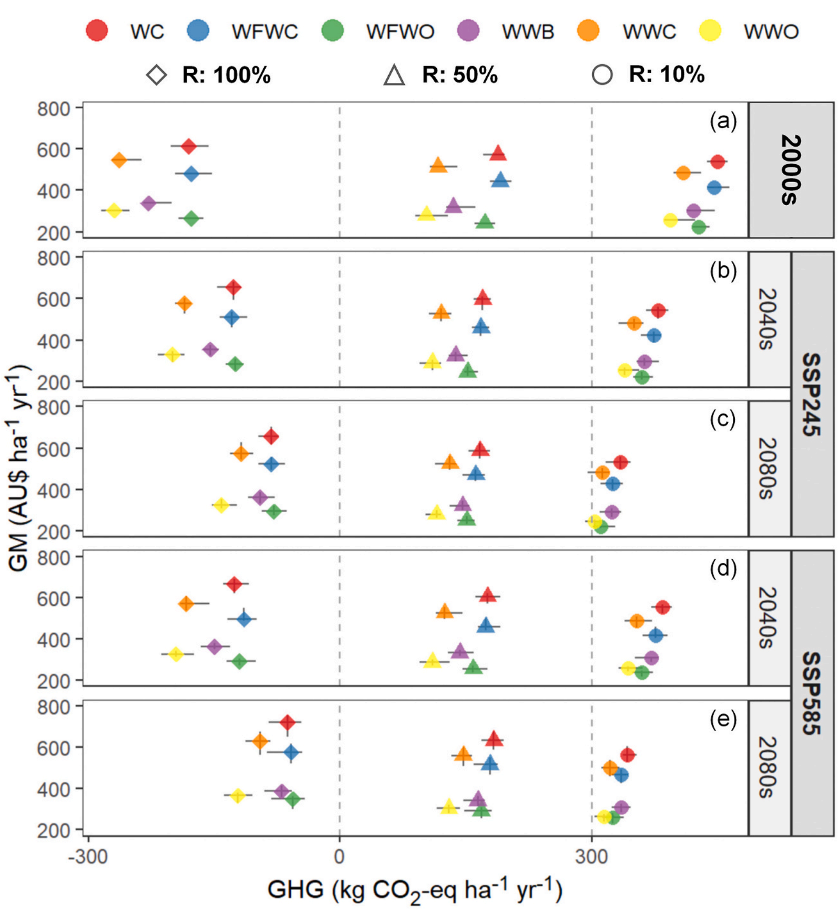

Fig. 4. Overall effect of management practices on relationships between GHG and GM during 2000s (a), 2040s (b and d) and 2080s (c and e) under SSP245 and SSP585 scenarios. Data are presented as the median values from APSIM simulations based on 27 GCMs. Horizontal and vertical error bars represent the 25th to 75th percentile range around the median for GHG and GM, respectively. The vertical dashed lines represent GHG emissions that are equal to 0 and 300 kg CO_2-eq ha^{-1} yr^{-1}, respectively. Crop rotation abbreviations are defined in Fig. 2.

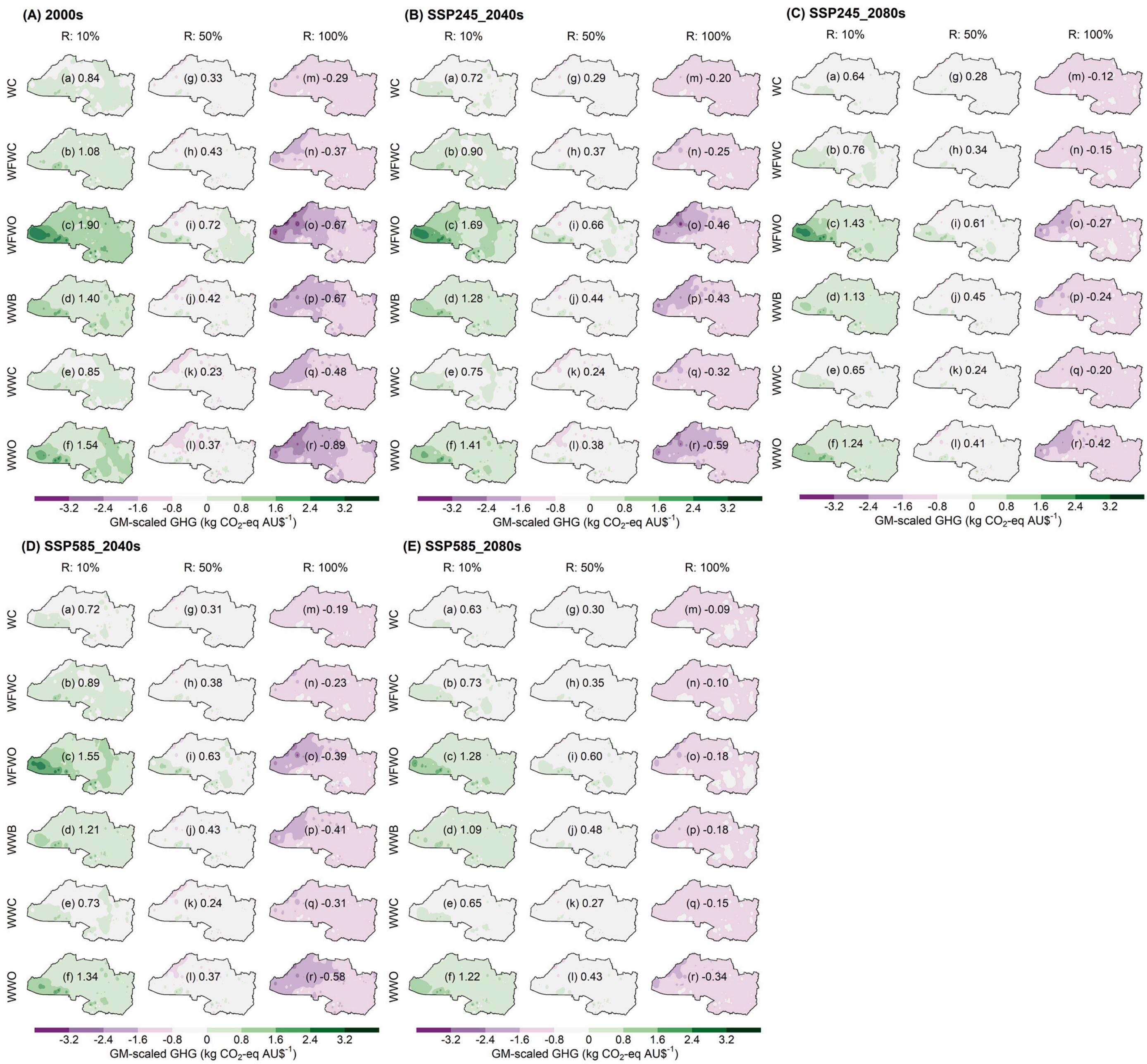

Fig. 5. Effects of management practices on the GM-scaled GHG (GHG/GM, kg CO_2-eq. AU$$^{-1}$) during 2000s (1985–2020), 2040s (2021–2056) and 2080s (2057–2092) under SSP245 and SSP585 scenarios across the study area. The spatial distributions of GHG/GM were interpolated using inverse distance weighting method (IDW) with median values from 27 GCMs. Numbers on the figure are spatial averages across the study region. Crop rotation abbreviations are defined in Fig. 2.

which SOC increases is related to the initial content (Farina et al., 2021; Xia et al., 2018; Zhao et al., 2013). Soils with a lower initial C content have a greater saturation deficit, which may result in a higher C sequestration rate and a longer duration to reach a new equilibrium (West and Six, 2007), depending on the extent to which management is changed from its original state (Henry et al., 2022).

Over the simulation period full residue retention increased SOC stocks, with the averaged SOC sequestration rates ranging from 77 kg C ha^{-1} yr^{-1} (2000s) to around 43 kg C ha^{-1} yr^{-1} (2080s) (Table S4). The sequestration rates are small in comparison to a study for the Australian wheat belt that reported an increase of soil C sequestration for 80–100 kg C ha^{-1} yr^{-1} by incorporating all straw into soil (Liu et al., 2014b), and are similar to results from Lugato et al. (2014) who reported an average SOC change rate for a cereal straw incorporation and reduced tillage scenario for EU-27 of 20–100 kg C ha^{-1} yr^{-1} from 2000 to 2050. It should be noted that the rates of soil C sequestration following total residue retention decreased after the first 80 years (around 2040), as a new C equilibrium was reached (Fig. 2m-r). The possible mechanism that might underpin the soil C saturation with long-term residue C input is that, the soil capacity to maintain organic C is regulated by the clay content (i.e., chemical stabilization), aggregation (i.e., physical protection) and recalcitrant compounds (i.e., bio-chemical stabilization) (Liu et al., 2014a). Dryland soils in Australia have greater C:N ratios than other land uses (Eldridge et al., 2018), which means that the crop stubble may have slower turnover rates into the SOC pool because of the relatively higher nitrogen demands of soil microorganisms (Jin et al., 2020). A meta-analysis in China showed that SOC responses were the greatest in the initial starting phase of straw incorporation but declined

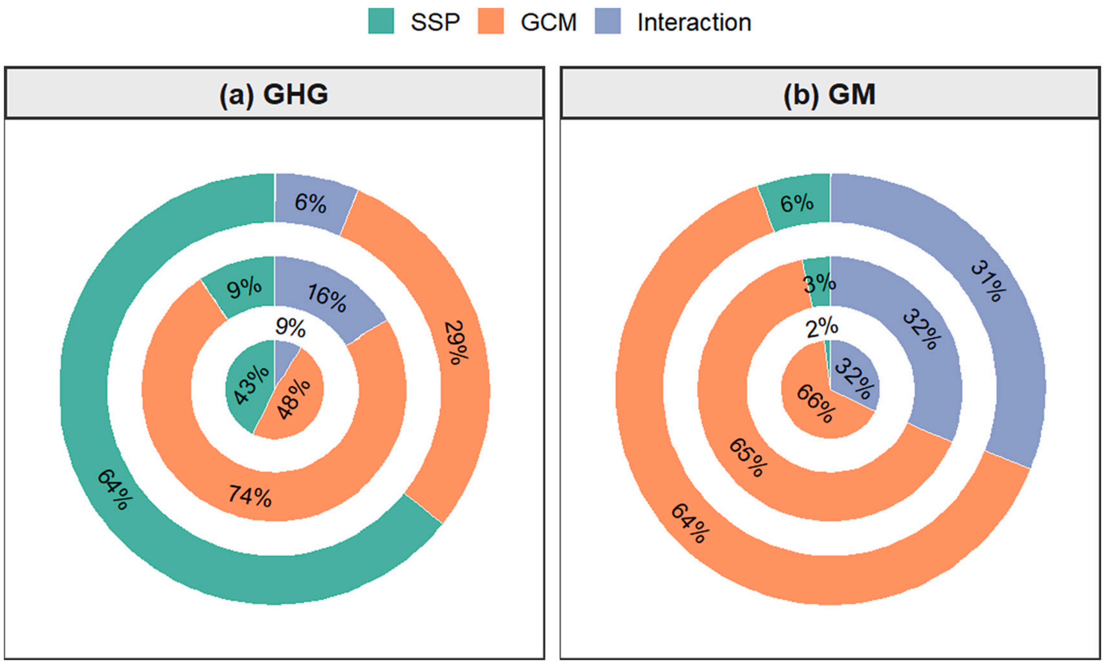

Fig. 6. Proportion of uncertainty in the simulated annual GHG (a) and GM (b) of WWC (wheat-wheat-canola) rotation. The sources of uncertainty were separated into SSP (e.g., SSP245_2040s, SSP245_2080s, SSP585_2040s, and SSP585_2080s), GCM, and their interaction. The inner-to-outer rings represent the uncertainty share for 10%, 50% and 100% residue retention, respectively.

after 28–62 years (Han et al., 2018), and a simulation study in south-east UK using RothC model found that the SOC accumulation rate declined after 50–100 years of cereal straw addition (Powlson et al., 2008).

4.2. Responses of N_2O emission to management practices

Although the soil GHG fluxes were dominated by SOC change, our results indicated a reduction in GHG removal potential due to the enhanced N_2O emissions when residues were retained (Fig. 2 m-r). The addition of crop residues increased SOC stocks by 38% on average, but the annual N_2O emissions also went up by 35% (Fig. S7), implying that crop residues supply N as a substrate for N_2O production (Abalos et al., 2022). The N_2O emissions for the whole simulated period ranged from 0.34 kg N ha^{-1} yr^{-1} for no residue retention to 0.46 kg N ha^{-1} yr^{-1} for 100% retention, which are considerably smaller than some previous studies (Table S7). Simulation results from Chen et al. (2019) showed that the average N_2O emissions on the Loess Plateau of China increased from 1.03 kg N ha^{-1} yr^{-1} (no straw) to 1.19 kg N ha^{-1} yr^{-1} (straw mulching) during 1981–2016 with a total 375 kg N ha^{-1} application. While fertilizer in this study ranged between 10 and 121 kg N ha^{-1} which may be one of the reasons for the small N_2O emissions. Myrgiotis et al. (2019) estimated the N_2O emissions of around 0.66, 0.49, and 4.80 kg N ha^{-1} yr^{-1} for barley, wheat, and oilseed rape cropping systems in eastern Scotland, suggesting the importance of N contained in crop residues on N_2O emissions. Li et al. (2017) reported lower N_2O emissions of 0.15–0.40 kg N ha^{-1} yr^{-1} from rotations including legume compared with 0.42–0.66 kg N ha^{-1} yr^{-1} from canola rotated with cereals under four RCP scenarios. Crop residues of cereals typically have higher C/N ratios (>40) than those of pulse crops, and thereby impact the substrate availability for nitrification and denitrification reactions (Wang et al., 2011). Moreover, the roots of cereal and pulse crops are generally distributed more evenly in the soil profile, while those of oilseed crops are accumulated more in the upper soil layers (Fan et al., 2016), which may also influence SOC inputs and N_2O emissions.

Crop residues, as the nutrient and energy resources for soil microbes, are subjected to microbial N mineralization and nitrification which result in N_2O production (Bilotto et al., 2021; Frimpong and Baggs, 2010), and meanwhile, they provide substrates for microbial growth and therefore increase SOC. There are some discrepancies between the results from different studies, which may be partly due to the different residue and fertilizer management. More importantly, these SOC and N_2O-related processes are parameterized in process-based models by using mathematical algorithms. Differences in model parameterization combined with different input datasets can be an important source of uncertainty across models and are still a great challenge (Tian et al., 2019). In this study, it should be pointed out that the soil C sequestration was compensated by accumulative N_2O emissions (in CO_2 equivalent) of 15–24% (for SSP245) and 16–28% (for SSP585) in 2080s when the soils reached an equilibrium with 100% residue retention (Fig. 2m-r and Table S4). This is in line with the results from Lugato et al. (2018), who reported that N_2O emissions from practices based on crop residue retention and lower soil disturbance would offset 13–47% of SOC gains (in CO_2 equivalent) by 2100 under the RCP4.5 scenario. A recent study using three biogeochemical models also found that the benefits of increased SOC sequestration by residue retention would eventually be compensated by N_2O emissions on the long run (50–100 years) (Haas et al., 2022). These results highlight that any strategy aiming at climate change mitigation in cropping systems should look at the coupled soil C sequestration and N_2O emissions together.

4.3. Responses of crop yield and gross margin to management practices

Apart from increasing soil SOC sequestration, residue retention also benefits crop yields (Table S8). Many studies have reported a positive correlation between SOC content and crop yield (Berhane et al., 2020; Han et al., 2018; Liu et al., 2014a). In this study, we found that residue retention increased or maintained yield of each crop in each rotation under both SSP245 and SSP585. Up to a point, crop growth benefits directly from increased soil organic matter (evidenced by higher SOC content) through the improvements in water and nutrient holding capacity, soil structure and biotic activity (Lal, 2004; Xia et al., 2018). Furthermore, the increased water use efficiency can enhance the resilience of agricultural production to climate change (Hao et al., 2020).

In Australia, most farmers are conscious of the weather-related risks to crop production (e.g., frost, flooding, and drought) and usually invest in practices based on economic optimum (Lam et al., 2013). Economic return is an important factor in farmers' decisions to adopt new management practices (Li et al., 2017; Meier et al., 2020a; Meier et al., 2017; Nash et al., 2013). Consistent with the above GHG and crop yield analysis, both increased GHG removal and increased gross margins were achieved under 100% residue retention (Fig. 3), which suggests that residue management provides an opportunity for economic and environmental co-benefits. In this study, we found that 100% residue retention increased gross margin by 22% on average compared with 10% retention (Table S6), which is consistent with the experimental findings of Li et al. (2021c) who reported that gross revenue increased by 22.1% with straw return, and the findings of Zhuang et al. (2019) who found that net profit increased by 53.4% with the combination of straw return and fertilizer optimization. The eastern region in Riverina had greater gross margins and higher GM-scaled GHG than the west (Fig. 5 and Fig. S5), suggesting that the eastern region would benefit less from residue retention.

Similar to results from Smith et al. (2013), we found that the wheat-canola rotation systems (WC and WWC) had high gross margins because canola price was high relative to other crops (Fig. 3B and Table 1). Leguminous rotations (WFWC and WFWO) were less profitable, which is contradictory to the findings of Xing et al. (2017) who reported that including legumes in cereal-based (wheat and canola) crop rotations were more profitable due to reduced N applications. The apparent discrepancy may be because our study applied 10 kg N ha^{-1} for field pea at sowing, and 43–121 kg N ha^{-1} for cereals and canola, without including the likely economic benefit of N contribution from legumes to subsequent crops. Southern Australia is characterized by a winter-dominated precipitation pattern, in which canola has become an important break crop for wheat-based rotations (Maaz et al., 2018). More importantly, the WWC combined with 100% residue retention can achieve both large gross margins and GHG abatement (Fig. 4), which may be closely linked to the quantity and quality of crop residues.

4.4. Climate change effect

A recent global meta-analysis reported that the climate drove SOC and crop yield changes under conservation agriculture (Sun et al., 2020). Our results show that climate change could hamper SOC accumulation as well as stimulate GHG emissions (Fig. 2). The negative effects were marginal compared with residue management practices, such as the 100% residue retention in which soils are always carbon sinks (Fig. 2m-r). However, taking the historical simulations as references, the annual GHG under 10% residue retention decreased with time for both SSP245 and SSP585 (Fig. 3A a-b). Generally, rates of chemical and microbial processes increase exponentially with temperature only when other factors (substrate or moisture availability) are not limiting (Meixner and Yang, 2006). The substrate (crop stubble in this study) under 10% retention would be exhausted with time and limiting GHG emissions, while for 100% retention, with large annual substrate addition, annual GHG emissions increased greatly in the future (Fig. 3A e-f). Moreover, the rainfall showed an increased trend in most parts of this study region (Fig. S8b and d), which may favor soil N_2O production (Chen et al., 2019; Schaufler et al., 2010; Wu et al., 2020).

Increased temperature, particularly during anthesis and grain filling, could result in decreased yields due to infertility and advanced maturity dates (Liu et al., 2020; Muleke et al., 2022). While elevated atmospheric CO_2 concentration can increase crop yields by enhancing photosynthetic rate and water use efficiency (Fitzgerald et al., 2016). Our results showed that the overall average crop yields for 2080s with 10% residue retention changed by −1.6% (wheat), −7.0% (oats), −5.7% (barley), +3.2% (canola) and + 16.0% (field pea) relative to the historical periods, and all the crop yield changes became positive, with increases of 4.7–14.7% for 100% residue retention (Table S8). This is consistent with the results from Liu et al. (2017), who suggested that residue incorporation could improve water use efficiency and mitigate the negative climate change impacts on crop yields. Interestingly, compared to canola and fieldpea, cereals (wheat, oats and barley) benefited more from residue retention shifting from negative response under 10% retention to positive under 100% retention, which may be partly due to their higher amounts of biomass (Flower et al., 2021). These results indicated that positive effects of residue retention on gross margins could overcome the adverse effects from climate change. However, the potential income from utilization of the crop residues removed under 10% and 50% retention scenarios was not considered in this study. Biomass can be used as livestock feed or bioenergy for climate change mitigation, but evaluating these scenarios requires more sophisticated modelling practices or life cycle assessment. The western part of Riverina region always had lower gross margins than the eastern part due to the hotter and drier climate (Fig. S5), suggesting a need to investigate a wider range of practices (e.g., pasture rotation, Meier et al. (2017)) and use of dry or heat tolerant cultivars to build a climate-resilient crop system in the future (Pequeno et al., 2021; Zhao et al., 2022).

4.5. Limitations and future research

We constrained our analysis to concentrate on the environmental and economic effects of management practices under climate change. There are still some limitations requiring additional research as well as providing insights into future studies. First, we did not consider the future fluctuation of on-farm prices and agrotechnology innovations (Schmidhuber and Tubiello, 2007). There are many factors influencing the crop yield and the subsequent price variability, such as pest or disease outbreaks, domestic policies, macro-economic conditions, and changing agrometeorology (Chatzopoulos et al., 2020), which need to be further assessed. Second, we aimed to evaluate the effectiveness of conservation farming practices, specifically residue retention and crop rotation, but did not consider the potential changes of these practices in the future. Although our N application rates are based on local practices and climate, and the six rotations comprised common rotation cycles across the Riverina, they are still simplified simulations of the real world. For example, breeding efforts may result in the adaptation of crops to climate change, and changes in social and other environmental factors may affect the choice of planting systems in the future. Therefore, the implications of the modelling results should be cautiously interpreted. In addition, although APSIM has been widely applied for agricultural management assessment globally, a single crop model may be overconfident. The uncertainties of GHG and gross margins from 27 GCMs were assessed (Figs. S4 and S6), but extending the simulation to a multi-model comparison with different model structures would provide additional information and greater confidence. Thus, a useful future extension would be to evaluate some other management options (e.g., fertilizer management, cover crop and green manure) based on conclusions from this study with multi-model ensembles to explore the mitigation and adaption potentials of management practices under climate change.

5. Conclusions

In this study, we conducted a comprehensive simulation analysis to quantify the interaction effects of crop rotation, residue retention, and climate change on both soil GHG emissions and gross margins at the regional level. Our results indicated that retaining all crop residues in cropland can turn the soil from a carbon source to a carbon sink, while the benefit was partly offset by the concomitantly increased N_2O emissions. The wheat-wheat-canola rotation with full residue retention could achieve a win-win solution with both large GHG abatement and high gross margin compared to other rotations. Spatial analysis showed the eastern Riverina region had higher gross margins while the western region had higher GHG abatement potentials. Climate change led to increased GHG emissions and decreased yields for some crops, but the adverse effects were smaller than the advantages provided from adopting residue conservation and wheat-wheat-canola rotation regarding the GHG abatement. The results from this study are expected to provide helpful information for farmers and policymakers to guide mitigation and adaptation strategies to meet the net-zero emission target of NSW government.

Declaration of Competing Interest

The authors declare that they have no known competing financial interests or personal relationships that could have appeared to influence the work reported in this paper.

Data availability

Data will be made available on request.

Acknowledgements

This study was funded by the NSW Primary Industries Climate Change Research Strategy, the NSW Climate Change Fund, and Natural Science Foundation of China (No. 41730645). KL and MTH were funded by Meat & Livestock Australia and the University of Tasmania (projects P.PSH.1219 and B.CCH.2121). We acknowledge the World Climate Research Programme, which, through its Working Group on Coupled Modelling, coordinated and promoted CMIP6. We thank the climate modelling groups for producing and making available their model output, the Earth System Grid Federation (ESGF) for archiving the data and providing access, and the multiple funding agencies who support CMIP6 and ESGF.

Appendix A. Supplementary data

Supplementary data to this article can be found online at https://doi.org/10.1016/j.agsy.2022.103527.

References

Abalos, D., Rittl, T.F., Recous, S., et al., 2022. Predicting field N2O emissions from crop residues based on their biochemical composition: a meta-analytical approach. Sci. Total Environ. 812, 152532.

Bai, H., Xiao, D., Wang, B., et al., 2022. Simulation of wheat response to future climate change based on coupled model inter-comparison project phase 6 multi-model ensemble projections in the North China plain. Front. Plant Sci. 13, 829580.

Berhane, M., Xu, M., Liang, Z., et al., 2020. Effects of long-term straw return on soil organic carbon storage and sequestration rate in North China upland crops: a meta-analysis. Glob. Chang. Biol. 26, 2686–2701.

Bilotto, F., Harrison, M.T., Rowlings, D.W., et al., 2021. Can seasonal soil N mineralisation trends be leveraged to enhance pasture growth? Sci. Total Environ. 772, 145031.

Butterbach-Bahl, K., Baggs, E.M., Dannenmann, M., et al., 2013. Nitrous oxide emissions from soils: how well do we understand the processes and their controls? Philos. Trans. R. Soc. B 368, 20130122.

Chang-Fung-Martel, J., Harrison, M.T., Rawnsley, R., et al., 2017. The impact of extreme climatic events on pasture-based dairy systems: a review. Crop Past. Sci. 68, 1158–1169.

Chatzopoulos, T., Domínguez, I.P., Zampieri, M., et al., 2020. Climate extremes and agricultural commodity markets: a global economic analysis of regionally simulated events. Weather Clim. Extrem. 27, 100193.

Chen, H., Li, L., Luo, X., et al., 2019. Modeling impacts of mulching and climate change on crop production and N2O emission in the loess plateau of China. Agric. For. Meteorol. 268, 86–97.

Choi, J., Ko, J., An, K.-N., et al., 2021. Simulation of staple crop yields for determination of regional impacts of climate change: a case study in Chonnam Province, Republic of Korea. Agronomy. 11, 2544.

Christie, K.M., Smith, A.P., Rawnsley, R.P., et al., 2020. Simulated seasonal responses of grazed dairy pastures to nitrogen fertilizer in SE Australia: N loss and recovery. Agric. Syst. 182, 102847.

Dalgliesh, N., Cocks, B., Horan, H., 2012. APSoil-providing soils information to consultants, farmers and researchers. In: Proceedings of the 16th ASA Conference. Armidale, Australia.

Del Grosso, S.J., Parton, W.J., Mosier, A.R., et al., 2000. General model for N2O and N2 gas emissions from soils due to dentrification. Glob. Biogeochem. Cycles 14, 1045–1060.

Department of Planning and Environment, 2017. Riverina Murray Regional Plan 2036, NSW Government. ISBN 978-1-76039-488-2.

Dumbrell, N.P., Kragt, M.E., Meier, E.A., et al., 2017. Greenhouse gas abatement costs are heterogeneous between Australian grain farms. Agron. Sustain. Dev. 37, 28.

Ehrhardt, F., Soussana, J.-F., Bellocchi, G., et al., 2018. Assessing uncertainties in crop and pasture ensemble model simulations of productivity and N2O emissions. Glob. Chang. Biol. 24, e603–e616.

Eldridge, D.J., Maestre, F.T., Koen, T.B., et al., 2018. Australian dryland soils are acidic and nutrient-depleted, and have unique microbial communities compared with other drylands. J. Biogeogr. 45, 2803–2814.

Fan, J., McConkey, B., Wang, H., et al., 2016. Root distribution by depth for temperate agricultural crops. Field Crop Res. 189, 68–74.

Farina, R., Sándor, R., Abdalla, M., et al., 2021. Ensemble modelling, uncertainty and robust predictions of organic carbon in long-term bare-fallow soils. Glob. Chang. Biol. 27, 904–928.

Feng, P., Wang, B., Liu, D.L., et al., 2020. Dynamic wheat yield forecasts are improved by a hybrid approach using a biophysical model and machine learning technique. Agric. For. Meteorol. 285-286, 107922.

Field, C.B., Mach, K.J., 2017. Rightsizing carbon dioxide removal. Science. 356, 706–707.

Fitzgerald, G.J., Tausz, M., O'Leary, G., et al., 2016. Elevated atmospheric [CO2] can dramatically increase wheat yields in semi-arid environments and buffer against heat waves. Glob. Chang. Biol. 22, 2269–2284.

Flower, K.C., Ward, P.R., Micin, S.F., et al., 2021. Crop rotation can be used to manipulate residue levels under no-tillage in a rainfed Mediterranean-type environment. Soil Tillage Res. 212, 105062.

Forster, P., Storelvmo, T., Armour, K., et al., 2021. The Earth's energy budget, climate feedbacks, and climate sensitivity. In: Climate Change 2021: The Physical Science Basis. Contribution of Working Group I to the Sixth Assessment Report of the Intergovernmental Panel on Climate Change. Cambridge University Press.

Frimpong, K.A., Baggs, E.M., 2010. Do combined applications of crop residues and inorganic fertilizer lower emission of N2O from soil? Soil Use Manag. 26, 412–424.

Godde, C.M., Thorburn, P.J., Biggs, J.S., et al., 2016. Understanding the impacts of soil, climate, and farming practices on soil organic carbon sequestration: a simulation study in Australia. Front. Plant Sci. 7, 661.

Grant, T., Cruypenninck, H., Eady, S., et al., 2014. AusAgLCI methodology for developing life cycle inventory. In: Rural Industries Research and Development Corporation. Publication No. 14/046.

Haas, E., Carozzi, M., Massad, R.S., et al., 2022. Long term impact of residue management on soil organic carbon stocks and nitrous oxide emissions from European croplands. Sci. Total Environ. 836, 154932.

Han, X., Xu, C., Dungait, J.A.J., et al., 2018. Straw incorporation increases crop yield and soil organic carbon sequestration but varies under different natural conditions and farming practices in China: a system analysis. Biogeosciences. 15, 1933–1946.

Hao, X., He, W., Lam, S.K., et al., 2020. Enhancement of no-tillage, crop straw return and manure application on field organic matter content overweigh the adverse effects of climate change in the arid and semi-arid Northwest China. Agric. For. Meteorol. 295, 108199.

Harrison, M.T., Cullen, B.R., Tomkins, N.W., et al., 2016. The concordance between greenhouse gas emissions, livestock production and profitability of extensive beef farming systems. Anim. Prod. Sci. 56, 370–384.

Harrison, M.T., Cullen, B.R., Mayberry, D.E., et al., 2021. Carbon myopia: the urgent need for integrated social, economic and environmental action in the livestock sector. Glob. Chang. Biol. 27, 5726–5761.

He, W., Grant, B.B., Jing, Q., et al., 2021. Measuring and modeling soil carbon sequestration under diverse cropping systems in the semiarid prairies of western Canada. J. Clean. Prod. 328, 129614.

Henry, B., Dalal, R., Harrison, M.T., et al., 2022. Creating frameworks to foster soil carbon sequestration. In: Burleigh Dodds Series in Agricultural Science. Oxford, UK.

Hergoualc'h, K., Akiyama, H., Bernoux, M., et al., 2019. N2O emissions from managed soils, and CO2 emissions from lime and urea application. In: Inventories E, Buendia, Calvo, et al. (Eds.), 2019 Refinement to the 2006 IPCC Guidelines for National Greenhouse Gas. Intergovernmental Panel on Climate Change, Geneva, pp. 11.11–11.48.

Hochman, Z., Horan, H., Garcia, J.N., et al., 2020. Cropping system yield gaps can be narrowed with more optimal rotations in dryland subtropical Australia. Agric. Syst. 184, 102896.

Huang, Y., Tao, B., Yang, Y., et al., 2022. Simulating no-tillage effects on crop yield and greenhouse gas emissions in Kentucky corn and soybean cropping systems: 1980-2018. Agric. Syst. 197, 103355.

Isbell, R.F., National Committee on Soil and Terrain, 2021. The Australian Soil Classification, 3rd edn. CSIRO Publishing, Melbourne.

Jeffrey, S.J., Carter, J.O., Moodie, K.B., et al., 2001. Using spatial interpolation to construct a comprehensive archive of Australian climate data. Environ. Model. Softw. 16, 309–330.

Jia, G., Shevliakova, E., Artaxo, P., et al., 2019. Land-climate interactions. In: Climate Change and Land: An IPCC Special Report on Climate Change, Desertification, Land Degradation, Sustainable Land Management, Food Security, and Greenhouse Gas Fluxes in Terrestrial Ecosystems [P.R. Shukla, J. Skea, E. Calvo Buendia, V. Masson-Delmotte, H.-O. Pörtner, D.C. Roberts, P. Zhai, R. Slade, S. Connors, R. van Diemen, M. Ferrat, E. Haughey, S. Luz, S. Neogi, M. Pathak, J. Petzold, J. Portugal Pereira, P. Vyas, E. Huntley, K. Kissick, M. Belkacemi, J. Malley, (eds.)]. In press.

Jin, Z., Shah, T., Zhang, L., et al., 2020. Effect of straw returning on soil organic carbon in rice-wheat rotation system: a review. Food Energy Secur. 9, e200.

Jin, N., Tao, B., Ren, W., et al., 2022. Assimilating remote sensing data into a crop model improves winter wheat yield estimation based on regional irrigation data. Agric. Water Manag. 266, 107583.

Keating, B.A., Carberry, P.S., Hammer, G.L., et al., 2003. An overview of APSIM, a model designed for farming systems simulation. Eur. J. Agron. 18, 267–288.

Kheir, A.M.S., Alkharabsheh, H.M., Seleiman, M.F., et al., 2021. Calibration and validation of AQUACROP and APSIM models to optimize wheat yield and water saving in arid regions. Land. 10, 1375.

Lal, R., 2004. Soil carbon sequestration impacts on global climate change and food security. Science. 304, 1623–1627.

Lam, S.K., Chen, D., Mosier, A.R., et al., 2013. The potential for carbon sequestration in Australian agricultural soils is technically and economically limited. Sci. Rep. 3, 2179.

Launay, C., Constantin, J., Chlebowski, F., et al., 2021. Estimating the carbon storage potential and greenhouse gas emissions of French arable cropland using high-resolution modeling. Glob. Chang. Biol. 27, 1645–1661.

Lehman, R.M., Osborne, S.L., Duke, S.E., 2017. Diversified no-till crop rotation reduces nitrous oxide emissions, increases soybean yields, and promotes soil carbon accrual. Soil Sci. Soc. Am. J. 81, 76–83.

Lehmann, J., Kleber, M., 2015. The contentious nature of soil organic matter. Nature. 528, 60–68.

Lessmann, M., Ros, G.H., Young, M.D., et al., 2021. Global variation in soil carbon sequestration potential through improved cropland management. Glob. Chang. Biol. 00, 1–16.

Li, Y., White, R., Chen, D., et al., 2007. A spatially referenced water and nitrogen management model (WNMM) for (irrigated) intensive cropping systems in the North China plain. Ecol. Model. 203, 395–423.

Li, G.D., Conyers, M.K., Schwenke, G.D., et al., 2016. Tillage does not increase nitrous oxide emissions under dryland canola (*Brassica napus* L.) in a semiarid environment of South-Eastern Australia. Soil Res. 54, 512–522.

Li, Y., Liu, D.L., Schwenke, G., et al., 2017. Responses of nitrous oxide emissions from crop rotation systems to four projected future climate change scenarios on a black Vertosol in subtropical Australia. Clim. Chang. 142, 545–558.

Li, G.D., Schwenke, G.D., Hayes, R.C., et al., 2018. Does 3,4-dimethylpyrazole phosphate or N-(n-butyl) thiophosphoric triamide reduce nitrous oxide emissions from a rain-fed cropping system? Soil Res. 56, 296–305.

Li, G.D., Schwenke, G.D., Hayes, R.C., et al., 2021a. Can legume species, crop residue management or no-till mitigate nitrous oxide emissions from a legume-wheat crop rotation in a semi-arid environment? Soil Tillage Res. 209, 104910.

Li, J., Wang, L., Luo, Z., et al., 2021b. Reducing N2O emissions while maintaining yield in a wheat-maize rotation system modelled by APSIM. Agric. Syst. 194, 103277.

Li, S., Hu, M., Shi, J., et al., 2021c. Integrated wheat-maize straw and tillage management strategies influence economic profit and carbon footprint in the Guanzhong plain of China. Sci. Total Environ. 767, 145347.

Liu, D.L., Zuo, H., 2012. Statistical downscaling of daily climate variables for climate change impact assessment over New South Wales, Australia. Clim. Chang. 115, 629–666.

Liu, D.L., Chan, K.Y., Conyers, M.K., 2009. Simulation of soil organic carbon under different tillage and stubble management practices using the Rothamsted carbon model. Soil Tillage Res. 104, 65–73.

Liu, C., Lu, M., Cui, J., et al., 2014a. Effects of straw carbon input on carbon dynamics in agricultural soils: a meta-analysis. Glob. Chang. Biol. 20, 1366–1381.

Liu, D.L., Anwar, M.R., O'Leary, G., et al., 2014b. Managing wheat stubble as an effective approach to sequester soil carbon in a semi-arid environment: spatial modelling. Geoderma. 214-215, 50–61.

Liu, D.L., O'Leary, G.J., Ma, Y., et al., 2016. Modelling soil organic carbon 2. Changes under a range of cropping and grazing farming systems in eastern Australia. Geoderma. 265, 164–175.

Liu, D.L., Zeleke, K.T., Wang, B., et al., 2017. Crop residue incorporation can mitigate negative climate change impacts on crop yield and improve water use efficiency in a semiarid environment. Eur. J. Agron. 85, 51–68.

Liu, K., Harrison, M.T., Hunt, J., et al., 2020. Identifying optimal sowing and flowering periods for barley in Australia: a modelling approach. Agric. For. Meteorol. 282-283, 107871.

Lugato, E., Bampa, F., Panagos, P., et al., 2014. Potential carbon sequestration of European arable soils estimated by modelling a comprehensive set of management practices. Glob. Chang. Biol. 20, 3557–3567.

Lugato, E., Leip, A., Jones, A., 2018. Mitigation potential of soil carbon management overestimated by neglecting N2O emissions. Nat. Clim. Chang. 8, 219–223.

Luo, Z., Wang, E., Sun, O.J., et al., 2011. Modeling long-term soil carbon dynamics and sequestration potential in semi-arid agro-ecosystems. Agric. For. Meteorol. 151, 1529–1544.

Luo, Z., Wang, E., Xing, H., et al., 2017. Opportunities for enhancing yield and soil carbon sequestration while reducing N2O emissions in rainfed cropping systems. Agric. For. Meteorol. 232, 400–410.

Maaz, T., Wulfhorst, J.D., McCracken, V., et al., 2018. Economic, policy, and social trends and challenges of introducing oilseed and pulse crops into dryland wheat cropping systems. Agric. Ecosyst. Environ. 253, 177–194.

Matthews, P., McCaffery, D., Jenkins, L., 2015. Winter Crop Variety Sowing Guide 2015. NSW Department of Primary Industries.

Mbow, C., Rosenzweig, C., Barioni, L.G., et al., 2019. Food security. In: Climate Change and Land: an IPCC special report on climate change, desertification, land degradation, sustainable land management, food security, and greenhouse gas fluxes in terrestrial ecosystems [P.R. Shukla, J. Skea, E. Calvo Buendia, V. Masson-Delmotte, H.-O. Pörtner, D.C. Roberts, P. Zhai, R. Slade, S. Connors, R. van Diemen, M. Ferrat, E. Haughey, S. Luz, S. Neogi, M. Pathak, J. Petzold, J. Portugal Pereira, P. Vyas, E. Huntley, K. Kissick, M. Belkacemi, J. Malley, (eds.)]. In press.

Meier, E.A., Thorburn, P.J., Kragt, M.E., et al., 2017. Greenhouse gas abatement on southern Australian grains farms: biophysical potential and financial impacts. Agric. Syst. 155, 147–157.

Meier, E., Lilley, J., Kirkegaard, J., et al., 2020a. Management practices that maximise gross margins in Australian canola (*Brassica napus* L.). Field Crop Res. 252, 107803.

Meier, E.A., Thorburn, P.J., Bell, L.W., et al., 2020b. Greenhouse gas emissions from cropping and grazed pastures are similar: a simulation analysis in Australia. Front. Sustain. Food Syst. 3, 121.

Meixner, F.X., Yang, W.X., 2006. Biogenic emissions of nitric oxide and nitrous oxide from arid and semi-arid land. In: D'Odorico, P., Porporato, A. (Eds.), Dryland Ecohydrology. Springer, Dordrecht, pp. 233–255.

Mielenz, H., Thorburn, P.J., Harris, R.H., et al., 2016. Nitrous oxide emissions from grain production systems across a wide range of environmental conditions in eastern Australia. Soil Res. 54, 659–674.

Mohanty, M., Sinha, N.K., Somasundaram, J., et al., 2020. Soil carbon sequestration potential in a vertisol in Central India- results from a 43-year long-term experiment and APSIM modeling. Agric. Syst. 184, 102906.

Muleke, A., Harrison, M.T., Voil, P.D., et al., 2022. Earlier crop flowering caused by global warming alleviated by irrigation. Environ. Res. Lett. 17, 044032.

Myrgiotis, V., Williams, M., Rees, R.M., et al., 2019. Estimating the soil N2O emission intensity of croplands in Northwest Europe. Biogeosciences. 16, 1641–1655.

Nash, D., Riffkin, P., Harris, R., et al., 2013. Modelling gross margins and potential N exports from cropland in South-Eastern Australia. Eur. J. Agron. 47, 23–32.

NGA, 2021. National Greenhouse Accounts Factors: 2021. Australian Government. Department of Industry, Science, Energy and Resources.

O'Leary, G.J., Liu, D.L., Ma, Y., et al., 2016. Modelling soil organic carbon 1. Performance of APSIM crop and pasture modules against long-term experimental data. Geoderma. 264, 227–237.

O'Neill, B.C., Tebaldi, C., van Vuuren, D.P., et al., 2016. The scenario model Intercomparison project (ScenarioMIP) for CMIP6. Geosci. Model Dev. 9, 3461–3482.

Paustian, K., Lehmann, J., Ogle, S., et al., 2016. Climate-smart soils. Nature. 532, 49–57.

Pequeno, D.N.L., Hernández-Ochoa, I.M., Reynolds, M., et al., 2021. Climate impact and adaptation to heat and drought stress of regional and global wheat production. Environ. Res. Lett. 16, 054070.

Powlson, D.S., Riche, A.B., Coleman, K., et al., 2008. Carbon sequestration in European soils through straw incorporation: limitations and alternatives. Waste Manag. 28, 741–746.

Probert, M.E., Dimes, J.P., Keating, B.A., et al., 1998. APSIM's water and nitrogen modules and simulation of the dynamics of water and nitrogen in fallow systems. Agric. Syst. 56, 1–28.

Quemada, M., Lassaletta, L., Leip, A., et al., 2020. Integrated management for sustainable cropping systems: looking beyond the greenhouse balance at the field scale. Glob. Chang. Biol. 26, 2584–2598.

Renwick, L.L.R., Deen, W., Silva, L., et al., 2021. Long-term crop rotation diversification enhances maize drought resistance through soil organic matter. Environ. Res. Lett. 16, 084067.

Richardson, C.W., Wright, D.A., 1984. WGEN: A Model for Generating Daily Weather Variables. ARS (USA).

Rodrigues, L., Hardy, B., Huyghebeart, B., et al., 2021. Achievable agricultural soil carbon sequestration across Europe from country-specific estimates. Glob. Chang. Biol. 00, 1–18.

Sándor, R., Ehrhardt, F., Grace, P., et al., 2020. Ensemble modelling of carbon fluxes in grasslands and croplands. Field Crop Res. 252, 107791.

Schaufler, G., Kitzler, B., Schindlbacher, A., et al., 2010. Greenhouse gas emissions from European soils under different land use: effects of soil moisture and temperature. Eur. J. Soil Sci. 61, 683–696.

Schmidhuber, J., Tubiello, F.N., 2007. Global food security under climate change. PNAS. 104, 19703–19708.

Simmons, A., Liu, D.L., Cowie, A., et al., 2022. Climate change mitigation potential of summer cowpea cover crops in southern Australian cropping systems is limited. Available at SSRN. https://doi.org/10.2139/ssrn.4102479.

Smith, E.G., Kutcher, H.R., Brandt, S.A., et al., 2013. The profitability of short-duration canola and pea rotations in western Canada. Can. J. Plant Sci. 93, 933–940.

Smith, P., Calvin, K., Nkem, J., et al., 2019. Which practices co-deliver food security, climate change mitigation and adaptation, and combat land degradation and desertification?*. Glob. Chang. Biol. 26, 1532–1575.

Sun, W., Canadell, J.G., Yu, L., et al., 2020. Climate drives global soil carbon sequestration and crop yield changes under conservation agriculture. Glob. Chang. Biol. 26, 3325–3335.

Thorburn, P.J., Probert, M.E., Robertson, F.A., 2001. Modelling decomposition of sugar cane surface residues with APSIM-residue. Field Crop Res. 70, 223–232.

Thorburn, P.J., Biggs, J.S., Collins, K., et al., 2010. Using the APSIM model to estimate nitrous oxide emissions from diverse Australian sugarcane production systems. Agric. Ecosyst. Environ. 136, 343–350.

Tian, H., Yang, J., Xu, R., et al., 2019. Global soil nitrous oxide emissions since the preindustrial era estimated by an ensemble of terrestrial biosphere models: magnitude, attribution, and uncertainty. Glob. Chang. Biol. 25, 640–659.

Wang, W., Dalal, R.C., Reeves, S.H., et al., 2011. Greenhouse gas fluxes from an Australian subtropical cropland under long-term contrasting management regimes. Glob. Chang. Biol. 17, 3089–3101.

Wang, B., Liu, D.L., O'Leary, G.J., et al., 2018a. Australian wheat production expected to decrease by the late 21st century. Glob. Chang. Biol. 24, 2403–2415.

Wang, G., Luo, Z., Wang, E., et al., 2018b. Reducing greenhouse gas emissions while maintaining yield in the croplands of Huang-Huai-Hai Plain, China. Agric. For. Meteorol. 260-261, 80–94.

Wang, B., Feng, P., Chen, C., et al., 2019a. Designing wheat ideotypes to cope with future changing climate in south-eastern Australia. Agric. Syst. 170, 9–18.

Wang, B., Liu, D.L., Evans, J.P., et al., 2019b. Modelling and evaluating the impacts of climate change on three major crops in South-Eastern Australia using regional climate model simulations. Theor. Appl. Climatol. 138, 509–526.

Wang, B., Feng, P., Liu, D.L., et al., 2020. Sources of uncertainty for wheat yield projections under future climate are site-specific. Nat. Food 1, 720–728.

Wang, B., Gray, J.M., Waters, C.M., et al., 2022. Modelling and mapping soil organic carbon stocks under future climate change in South-Eastern Australia. Geoderma. 405, 115442.

West, T.O., Six, J., 2007. Considering the influence of sequestration duration and carbon saturation on estimates of soil carbon capacity. Clim. Chang. 80, 25–41.

Wood, T., Reeve, A., Ha, J., 2021. Towards Net Zero: Practical Policies to Reduce Agricultural Emissions. https://grattan.edu.au/report/towards-net-zero-practical-policies-to-reduce-agricultural-emissions/.

Wu, G., Chen, X., Ling, J., et al., 2020. Effects of soil warming and increased precipitation on greenhouse gas fluxes in spring maize seasons in the North China plain. Sci. Total Environ. 734, 139269.

Xia, L., Lam, S.K., Wolf, B., et al., 2018. Trade-offs between soil carbon sequestration and reactive nitrogen losses under straw return in global agroecosystems. Glob. Chang. Biol. 24, 5919–5932.

Xing, H., Liu, D.L., Li, G., et al., 2017. Incorporating grain legumes in cereal-based cropping systems to improve profitability in southern New South Wales, Australia. Agric. Syst. 154, 112–123.

Yan, Z., Zhang, X., Rashid, M.A., et al., 2020. Assessment of the sustainability of different cropping systems under three irrigation strategies in the North China plain under climate change. Agric. Syst. 178, 102745.

Yang, Y., Liu, D.L., Anwar, M.R., et al., 2016. Water use efficiency and crop water balance of rainfed wheat in a semi-arid environment: sensitivity of future changes to projected climate changes and soil type. Theor. Appl. Climatol. 123, 565–579.

Zhao, G., Bryan, B.A., King, D., et al., 2013. Impact of agricultural management practices on soil organic carbon: simulation of Australian wheat systems. Glob. Chang. Biol. 19, 1585–1597.

Zhao, Z., Wang, E., Kirkegaard, J.A., et al., 2022. Novel wheat varieties facilitate deep sowing to beat the heat of changing climates. Nat. Clim. Chang. 12, 291–296.

Zhuang, M., Zhang, J., Lam, S.K., et al., 2019. Management practices to improve economic benefit and decrease greenhouse gas intensity in a green onion-winter wheat relay intercropping system in the North China plain. J. Clean. Prod. 208, 709–715.